Deep Ocean Response to Hurricanes as Revealed by an Ocean Model with Free Surface. Part I: Axisymmetric Case

SIMON W. CHANG

Naval Research Laboratory, Washington, DC 20375

(Manuscript received 1 September 1984, in final form 12 July 1985)

ABSTRACT

An axisymmetric, hydrostatic ocean model containing a rigid bottom and a free surface is constructed to study the barotropic and baroclinic response in the upper and deep ocean to a wind stress corresponding to a stationary tropical cyclone. The numerical model covers a domain of 800 km and 1475 m in r- and z-directions, respectively, with a uniform radial resolution of 20 km and a stretched vertical resolution from 5 to 54 m. The vertical mixing is parameterized based on a local Richardson number and a mixing length.

The model ocean is spun up with the wind stress of Hurricane Eloise. A strong tangential circulation develops that extends to the ocean floor with a maximum speed of 1.2 m s^{-1} at the surface. The circulation on the r–z plane, which also extends to the ocean floor, oscillates with time with a maximum upwelling of 0.1 cm s^{-1} at the center. Surface height has a maximum depression of 57 cm. The deep overturning causes density changes deep in the ocean. A maximum temperature decrease of 3°C occurs in the mixed layer at the center; a maximum temperature increase of 0.45°C is found just below the thermocline at a radius of 200 km. The recovery of both the mass and momentum fields is very slow during the spindown. Inertial oscillations dominate in the spindown even in the deep ocean. Adjustments between the momentum and mass fields seem to converge to a state quite different from the prestorm state.

Direct comparison with observations is difficult because the model is only two-dimensional. Nevertheless, recent observations seem to suggest the existence of the barotropic response in the deep ocean. The model suggests that the observed rapid response in the deep ocean is caused by the barotropic pressure gradient force, which arises from the storm-induced perturbation of the free surface.

1. Introduction

The response of the ocean to tropical cyclones has been studied with pure baroclinic models, pure barotropic models and linear models that consider both the baroclinic and barotropic responses. In all of the baroclinic models (e.g., O'Brien and Reid, 1967; Gilbert, 1972; Elsberry *et al.*, 1976; Chang and Anthes, 1978, 1979; Price, 1981; Greatbatch, 1983; Gill, 1984), the barotropic part of the response was excluded for numerical reasons. That is, the ocean surface in these models is flat. The advantage of excluding the barotropic part of the response is that the models can be integrated with larger time steps. The ocean's response was assumed to occur in one (such as in Chang and Anthes, 1978) or several (such as in Price, 1981) stratified layers near the surface. In addition, it was assumed that the bottom layer was infinitely deep and perpetually at rest. The hurricane-induced barotropic response as well as the response in the deep ocean below the mixed layer cannot be properly simulated in these baroclinic models. In the barotropic studies (e.g., Sugihara, 1973; Kuo and Ichiye, 1977), the ocean response is represented in only one or two model layers; therefore, vertical details of the response are not simulated. In linear models that include both the baroclinic and barotropic responses (e.g., Geisler, 1970), the barotropic and baroclinic modes are treated separately and there is no dynamical interaction between them.

Recent observations have shown that the ocean response to tropical cyclones is not restricted to the upper ocean. For example, Pudov *et al.* (1978) showed that the ocean water from a depth of 240 m was upwelled near the track of Typhoon Tess (1975). Hurricane Frederic induced ocean currents at least as deep as 450 m (Hopkins, 1982). The onset of the deep current has little or no time lag from the surface response, which implies that vertical turbulent mixing cannot be responsible for its occurrence. Shay and Elsberry (1986) found that the barotropic part constituted an important portion in the response of the ocean to Hurricane Frederic. They showed that the variance in the wake contributed by the barotropic mode was larger than that by the baroclinic modes in the wake. Brooks (1983) concluded that the vertical scale of ocean response in the Gulf of Mexico after Hurricane Allen of 1980 is much larger than the depth of the thermocline of 200 m. These findings warrant a reexamination of the ocean's baroclinic as well as barotropic response to tropical cyclones.

In this study, the ocean response to hurricane winds is studied with an ocean model that includes the baro-

tropic mode and which still has good vertical resolution for the baroclinic response. As shown by Chang and Anthes (1978, 1979), the three-dimensional response of the ocean to passing hurricanes is quite different from the two-dimensional axisymmetric response. The comparison of the axisymmetric result with observations may be difficult. However, as the first step toward the understanding of the deep ocean response, we are only concerned in this paper with the axisymmetric response. The more realistic three-dimensional response of the ocean to moving tropical cyclones will be presented in a forthcoming paper.

2. Numerical model

In this section, we first list the basic equations of the model. The splitting of the barotropic and the baroclinic modes in the basic equations and the parameterization of the vertical turbulent mixing will then be discussed. This will be followed by a brief review of the finite difference and the split–explicit integration method.

a. Basic equations

The basic equations describing an axisymmetric, hydrostatic and incompressible fluid as shown in Fig. 1 are

$$\frac{\partial u}{\partial t} = A - \frac{1}{\rho_0}\frac{\partial p}{\partial r} \tag{1}$$

$$\frac{\partial v}{\partial t} = B \tag{2}$$

$$\frac{\partial \rho}{\partial t} = C \tag{3}$$

$$\frac{1}{r}\frac{\partial ru}{\partial r} + \frac{\partial w}{\partial z} = 0 \tag{4}$$

$$\frac{\partial p}{\partial z} = -\rho g \tag{5}$$

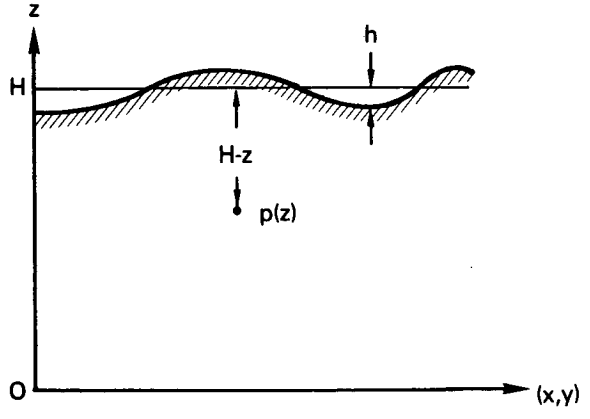

FIG. 1. Structure of the ocean model with a mean depth of H and a free surface.

where

$$A = -u\frac{\partial u}{\partial r} - w\frac{\partial u}{\partial z} + \frac{v^2}{r} + fv + K_H\left(\nabla^2 u - \frac{u}{r^2}\right) + \frac{\partial}{\partial z}K_Z\frac{\partial u}{\partial z} \tag{1a}$$

$$B = -u\frac{\partial v}{\partial r} - w\frac{\partial v}{\partial z} - \frac{uv}{r} - fu + K_H\left(\nabla^2 v - \frac{v}{r^2}\right) + \frac{\partial}{\partial z}K_Z\frac{\partial v}{\partial z} \tag{2a}$$

$$C = -u\frac{\partial \rho}{\partial r} - w\frac{\partial \rho}{\partial z} + K_H\nabla^2\rho + \frac{\partial}{\partial z}K_Z\frac{\partial \rho}{\partial z}. \tag{3a}$$

In the above equations, K_H and K_Z denote turbulent eddy diffusivities in the horizontal and vertical directions, respectively. The operator ∇^2 is defined as

$$\nabla^2 = \frac{\partial}{\partial r^2} + \frac{1}{r}\frac{\partial}{\partial r}.$$

b. Barotropic and baroclinic modes

The hydrostatic pressure at the depth of $d = H - z$ in the fluid is equal to the weight of the fluid above, i.e.,

$$p(z) = g\int_z^{H+h}\rho dz' = g\int_z^{H}\rho dz' + g\int_H^{H+h}\rho dz' \tag{6}$$

where H is the undisturbed mean height of the fluid, and h is the perturbation of the fluid surface from H and $h \ll H$. The value of $p(z)$ defined by (6) contains a large portion of the reference weight $\rho_0 g(H - z)$, which does not contribute to the pressure gradient, where ρ_0 is a reference density of the fluid (1.035 g cm^{-3}). We now define a relative pressure

$$p_r(z) = p(z) - g\rho_0(H - z) \quad \text{so that}$$

$$\frac{\partial}{\partial r}p_r(z) = \frac{\partial}{\partial r}p(z).$$

Let any first moment quantity be expressed as the sum of a vertical mean and a perturbation from the mean, i.e., $(\ ) = [\ ] + (\ )'$, where

$$[\ ] = \frac{1}{H}\int_0^H (\ )dz. \tag{7}$$

Defining the density deviation $\epsilon = \rho - \rho_0$, it can be shown that

$$p_r(z) = g[\epsilon](H - z) + g\int_z^H \epsilon' dz' + \rho_s g h \tag{8}$$

where ρ_s is the fluid density at the surface. Here it is assumed that the vertical variation of density over the depth of h is negligible because h is small. It is obvious that the last term in (8), which is due to perturbations

in free surface, exerts a pressure force on the whole water column and is independent of z. To calculate the reference pressure that acts on the water column, we apply the operator defined by (7) to (8),

$$[p_r] = \frac{1}{2}[\epsilon]gh + g[\epsilon' z] + \rho_s gh \tag{9}$$

$$p_r' = p_r - [p_r]. \tag{10}$$

The vertical-mean pressure gradient force (PGF), $\partial[p_r]/\partial r$ exerts the same force throughout the column, and therefore excites the vertical-mean motion, or the barotropic mode in the fluid. The perturbation PGF, $\partial p_r'/\partial r$, generates no mean acceleration and therefore only excites the baroclinic mode. Following the same method, Eqs. (1)–(3) can also be separated into these two modes. The equations for the barotropic mode are

$$\frac{\partial[u]}{\partial t} = [A] - \frac{1}{\rho_0}\frac{\partial}{\partial r}[p_r] \tag{11}$$

$$\frac{\partial[v]}{\partial t} = [B] \tag{12}$$

$$\frac{\partial[\epsilon]}{\partial t} = [C], \tag{13}$$

and the equations for the baroclinic mode are

$$\frac{\partial u'}{\partial t} = A' - \frac{1}{\rho_0}\frac{\partial}{\partial r}p_r' \tag{14}$$

$$\frac{\partial v'}{\partial t} = B' \tag{15}$$

$$\frac{\partial \epsilon'}{\partial t} = C'. \tag{16}$$

Now the two equation sets for the two modes are complete except for a prognostic equation for the free surface h, which enters in (8) and (9). Assuming the vertical motion $w = 0$ at the ocean floor $z = 0$, and integrating the continuity equation (4), we get

$$\int_0^{H+h}\frac{\partial w}{\partial z}\,dz = w(H+h) - w(0) = w(H+h)$$

$$= -\int_0^{H+h}\frac{1}{r}\frac{\partial ru}{\partial r}\,dz = -\frac{H}{r}\frac{\partial r[u]}{\partial r} - \frac{h}{r}\frac{\partial ru_s}{\partial r}.$$

Thus the prognostic equation for h is

$$\frac{\partial h}{\partial t} = -\frac{H}{r}\frac{\partial r[u]}{\partial r} - \frac{h}{r}\frac{\partial ru_s}{\partial r} - u_s\frac{\partial h}{\partial r}. \tag{17}$$

We have now only separated the basic equation set into a barotropic mode and a baroclinic mode. For typical ocean stratification, the characteristic speed of the former is approximately 100 times faster than that of the latter. Therefore a time step of ~100 of that allowed for the barotropic mode can be used for integrating the baroclinic mode. Madala and Piascek (1977) further separated the baroclinic mode into internal normal modes and used a semi-implicit method to solve their equations. Gill (1984) also solved his linear equation set by splitting normal modes, but the barotropic mode was neglected. Notice that we have neglected the atmospheric pressure force in (6), which acts on the whole water column and generates a barotropic response. Its effects are well understood in linear models. In supplementary experiments, the response of this ocean model to the atmospheric pressure forcing of a typical hurricane consisted of a bulged surface near the center and negligibly weak circulations. To avoid unnecessary masking of the wind-induced response, I choose to neglect the effect of the atmospheric pressure altogether.

The barotropic set of equations (11)–(13) are in fact the same as in linear models where barotropic response is treated independently from the baroclinic response (Kajiura, 1956; Geisler, 1970; Kuo and Ichiye, 1977). However, the barotropic mode in this model can interact with the baroclinic mode. Thus, baroclinic forcing can induce a barotropic response, and vice versa. The dynamical links between the two modes are provided by terms A, B and C, which appear on the rhs in both sets of equations, (11)–(13) and (14)–(16).

c. *Vertical mixing*

Various parameterizations of the vertical turbulent mixing have been used in modeling the ocean response to tropical cyclones. O'Brien and Reid (1967) parameterized the vertical mixing by a Raleigh friction formulation. Chang and Anthes (1978) considered the energy needed for the entrainment of the denser deep ocean water into the mixed layer to be completely supplied by the wind stress at the surface. Elsberry *et al.* (1976) used a similar formulation except that the available turbulent energy had an exponential decay in depth. Price (1981) and Greatbatch (1983) utilized a closure scheme based on the bulk Richardson number of the mixed layer. In all of these models, mixing was assumed to take place between stratified layers. The vertical resolutions were poor, and it was difficult to relate the vertical motions between stratified layers to upwelling.

In this model, vertical resolution in the mixed layer is 5–10 m, and the mixing is calculated between grid points. We selected a eddy diffusivity based on a mixing length and a local Richardson number. The vertical eddy diffusion coefficient K_Z is defined

$$K_Z = \begin{cases} (1 - \mathrm{Ri})^{1/2}\left[\left(\dfrac{\partial u}{\partial z}\right)^2 + \left(\dfrac{\partial v}{\partial z}\right)^2\right]^{1/2} l^2, & \text{for Ri} < 1 \\ 0, & \text{for Ri} \geqslant 1 \end{cases} \tag{18}$$

where the local Richardson number Ri is

$$\mathrm{Ri} = -\frac{g/\rho_0\,\partial\epsilon'/\partial z}{(\partial u/\partial z)^2 + (\partial v/\partial z)^2} \tag{19}$$

and l is the mixing length. In the above, a critical Ri of 1 and a turbulent Prandtl number of 1 are assumed. It can be argued that these numbers could assume other values. While further refinements may lead to improvement, this simple parameterization is sufficient to yield reasonable results.

There are a number of ways to define the mixing length l. Here we simply let l equal to the depth below the surface, which implies that the depth of the well-mixed layer (Ri < 1) is the scale of the eddy. Again, further refinement and verification with observations are left for future study. The K-coefficient defined in (18), combined with vertical gradients of velocity components and density, forms the vertical fluxes in the last terms in (1a)–(3a). Vertical fluxes are assumed to be zero at the top and bottom boundary, except the specified wind stress at the surface.

d. *Grid, finite difference formulation and temporal integration*

The model grid is illustrated in Fig. 2 where a uniform horizontal resolution of 20 km is used. In the vertical, the grid is stretched. The vertical distance between two adjacent points is progressively increased downward by a factor of 0.2. The vertical resolution is 5 m just below the surface and decreases to 54 m near the ocean floor. There are 41 × 51 grid points in the model, which covers 800 km and 1475 m in the radial and vertical directions, respectively.

The details of the finite difference formulation and the split–explicit integration method are given in Chang (1984), so that only a brief review is presented here. As shown in Fig. 2, the grid is fully staggered as the Arakawa C grid. Spatial differences are centered, and the advection terms are second-order accurate. The barotropic and baroclinic sets of equations are integrated separately by a leapfrog scheme with two different time steps. The time intervals are 30 and 1200 s, respectively. A horizontal diffusion coefficient of 10^5 cm^2 s^{-1} is used for numerical smoothing.

The computation cycle starts with the evaluation of terms A, B and C defined as the rhs of Eqs. (1)–(3), except for the PGF term in (1). Then vertical integrations are carried out to obtain $[A]$, $[B]$ and $[C]$. The next step is to integrate the barotropic set of equations (11)–(13) and (17) for 40 times with a 30 s interval. Notice here that the vertical-mean PGF is updated each time with a new h. The values of $[A]$, $[B]$ and $[C]$ remain constant during these 40 steps, by which a great computational economy is achieved. The baroclinic set of equations (14)–(16) is then integrated once, followed by evaluations of the hydrostatic pressure and the vertical motion by (4).

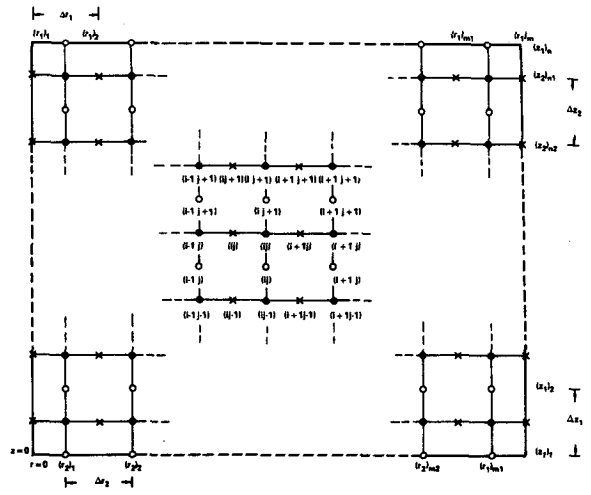

FIG. 2. Structure of the staggered grid. Horizontal velocities are defined at x points, vertical velocities are defined at circle points and pressures and densities are defined at dot points.

e. *Surface wind stress and initial stratification*

The response of the ocean to hurricanes is very sensitive to the characteristics of the surface wind and the prestorm stratification in the ocean. As summarized in Black (1983), the maximum ocean surface temperature (OST) changes vary from −1 to −6°C with different storms and oceans. We here select the case of Hurricane Eloise (1975) as the boundary forcing and buoy EB-10 data for the initial conditions. In the composite tangential wind in Hurricane Eloise (Price, 1981), there is a maximum of 32 m s^{-1} at r = 40 km and fairly rapid decay outward to 10 m s^{-1} at r > 450 km. There are several second-order discontinuities in the radial distribution of the tangential wind, notably one at 530 km. Because of the uncertainty in the composite radial wind, we let the radial wind component be one-half of the tangential wind. The 30 deg inflow angle assumed here appears to be quite large. However, the composite inflow angle ranges from 20 deg at r = 50 km to 30–45 deg at r > 120 km. Considering the large scatter in the composite radial velocity, the 30 deg angle seems to be a good compromise. A constant drag coefficient of 0.003 is used to compute the surface wind stress. A number of supplementary experiments have been conducted to test the model's sensitivity to the inflow angle and drag coefficient. While different parameters produce numerically different results, model results vary within a very reasonable range and are essentially similar to the result presented here.

The EB-10 sounding on 20 September 1975 is used as the initial condition for our computations. Buoy EB-10 provides temperature readings at depths of 2, 53, 220 and 530 m. A linear interpolation is performed to specify initial densities at model points, except that an initial thermocline of 30 m is artificially introduced. The initial density field is homogeneous and the ocean

is at rest. There is no initial perturbation in the free surface height. In the model computation, no attempt is made to differentiate contributions from temperature or salinity to density changes. Effects of evaporation, precipitation and sensible air–sea heat exchange are also neglected. The Coriolis parameter is set constant equal to the value for 30°N.

3. Spinup

The numerical integration of the model is started with the sudden imposition of the surface wind stress, which is then held constant for 48 h. The computations are continued for an additional 96 h without the surface wind stress to show the recovery in the ocean model. Sudden imposition and termination of wind stress may cause inertial oscillations with large amplitude (Gilbert, 1972). However, to apply a gradual increasing wind stress to the axisymmetric ocean can only simulate the rare situation associated with intensifying *and* stationary hurricanes.

a. Momentum field

Under the strong stress, the surface tangential velocity is generated quickly and grows to a maximum after 6 h. The maximum surface tangential velocity of more than 1.2 m s^{-1} occurs at the radius of the maximum stress of 60 km and remains nearly unchanged throughout the forcing period. It seems that the acceleration by the wind stress and the downward momentum transfer by mixing reached a balance at that velocity. Below the surface, the tangential circulation steadily develops, as shown by Fig. 3.

The high tangential current speeds are mainly restricted in the mixed layer, which deepens in time outside the radius of the maximum stress. There are large vertical shears at the top of the thermocline and only moderate shears in the mixed layer. The current just below the thermocline outside the central upwelling region is anticyclonic. This anticyclonic flow first appears at 12 h when the density field is modified to yield a pressure field similar to a "high" in that region. The strength of the anticyclonic flow oscillates at roughly the inertial period.

In the deep ocean, a tangential current forms without vertical shear with a maximum of 6.5 cm s^{-1} at $r = 100$ km at 24 h. It grows to 13.5 cm s^{-1} at 48 h. The deep cyclonic circulation, which extends all the way to the ocean floor, is mainly the barotropic response to the surface wind stress. In supplementary experiments (not shown here), in which the depth of the ocean H is altered, the deep cyclonic current still occupies the whole water column. It is mainly because the PGF, arising from the variations of h, acts on the whole column. We will discuss the barotropic response, including the changes in h, in a section to follow.

Figure 4 shows the circulation in the r–z plane at 12, 24, 36 and 48 h expressed in terms of the streamfunction ψ,

$$\psi = r \int_0^z u dz'. \tag{20}$$

The hurricane stress induces a vertical circulation that includes a concentrated upwelling at small radii and a broad weak downwelling at large radii. Deep upwelling near the storm path after tropical cyclones has been observed and discussed in Pudov *et al.* (1978) and Brooks (1983). The circulation in the radial direction features strong outflow in the mixed layer and gentle returning inflow between the thermocline and the ocean floor. In supplementary experiments in which the static stability is increased below 1000 m, the deep turning-over persists, albeit slightly compressed in the vertical. Figure 5 shows the vertical velocity at the depth of 56 m near the center. The maximum velocity varies between 0.09 and 0.11 cm s^{-1} during the spinup period.

Outside the central region of concentrated deep upwelling, the r–z circulation is oscillatory. The circulation is stronger at 12 and 36 h and weaker at 24 and 48 h. Corresponding to the oscillation, the maximum vertical velocity also varies, as shown in Fig. 5. The oscillation at large radii is to a certain extent caused by the sudden imposition of the wind stress. The oscillation at the inertial period also appeared in O'Brien (1967) and Chang and Anthes (1979), and was examined by Gilbert (1972) in detail. The inertial oscillation is illustrated by the current vectors every 6 h at $r = 180$ km at a depth of 90 m in Fig. 6. The current has an inertial oscillation at a period of about one day with a magnitude of 18 cm. A gradual increase of the tangential velocity is clearly superposed on the oscillation. There is observational evidence that Hurricane Frederic (1979) has caused a deep and oscillatory response in the Gulf of Mexico (Hopkins, 1982; Shay and Elsberry, 1985). Hopkins shows the water trajectory for 7–18 September 1979 at a depth of 251 m and at one degree longitude to the right of the storm track. Quite similar to the current vectors in Fig. 6, the observed trajectory consists of a mean current and an inertial motion, which was storm-induced. There is little time lag between the upper and deep ocean response.

The response in the deep ocean shown here has never been revealed in earlier baroclinic model studies because the deep bottom layers have been assumed to be motionless (to remove the barotropic mode) in these models. Because the depth of the model mixed layer at this radius never reaches 100 m, the vertical mixing of momentum obviously cannot produce motions at depths greater than 100 m. Only the barotropic PGF can "transmit" the upper ocean changes immediately to the bottom water. Although the model is axisymmetric, in the absence of other plausible mechanisms responsible for the observed deep ocean response, the barotropic PGF is conjectured to be the cause of the deep ocean response.

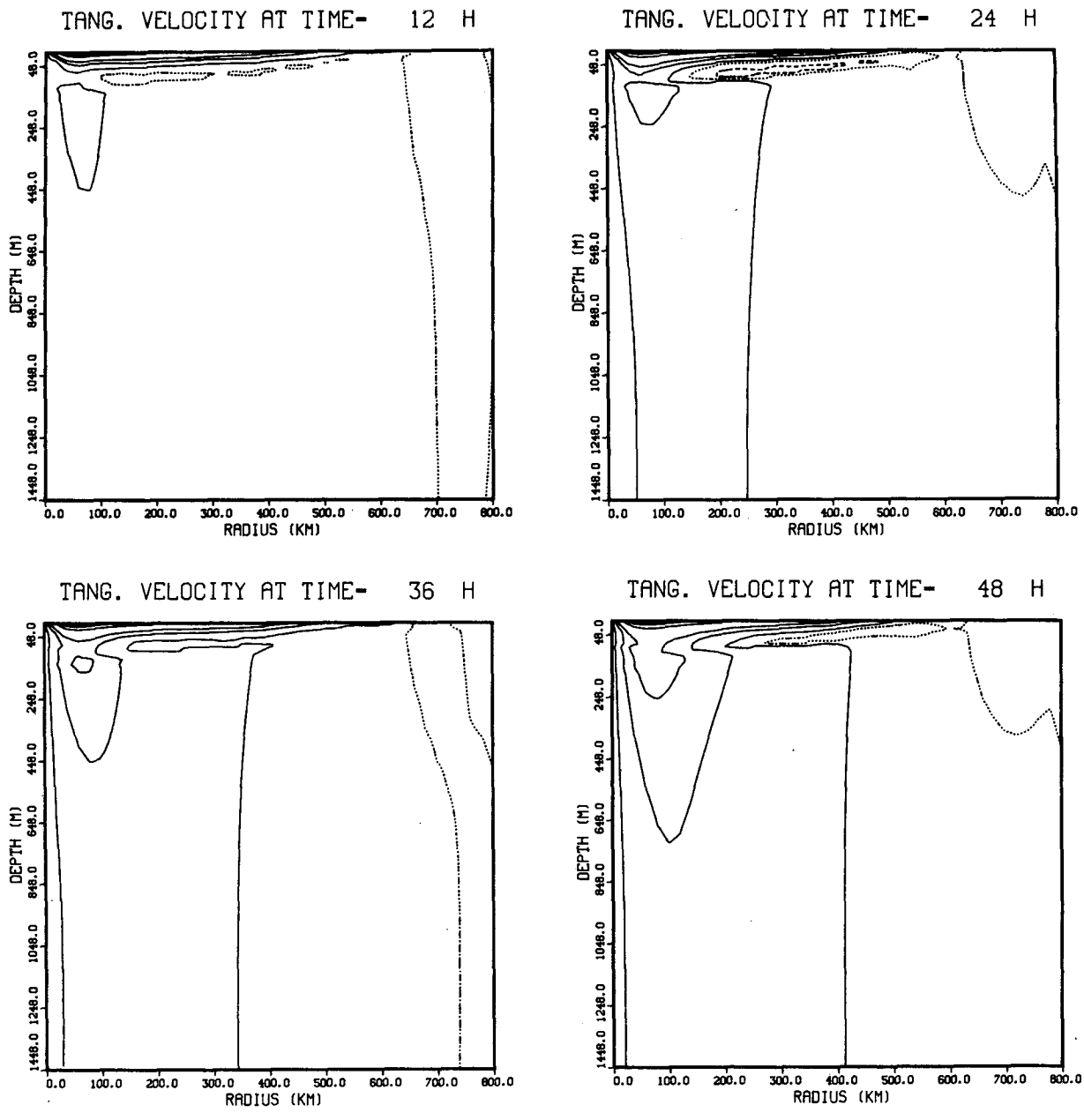

FIG. 3. Tangential velocities at 12, 24, 36 and 48 h. Contours have values of −10, −5, 0, 10, 20, 60, 100, 140, 180 and 220 cm s^{-1}. Solid lines denote positive contours (cyclonic tangential current); dashed lines, negative contours (anticyclonic tangential current); and dotted lines are for zero value.

b. Density field

The density field is modified to a great extent by the induced vertical mixing in the shallow ocean and by overturning in the deep ocean. Most of the density change in the early hours occurs in the mixed layer and is mainly produced by vertical mixing (Fig. 7). For example, at 6 h, the maximum density increase (or temperature decrease) occurs in the middle of the mixed layer at a depth of 22 m, and the maximum decrease (or temperature increase) occurs below the thermocline at a depth of 50 m, both at the radius of the maximum stress. There are only small density changes in the deep ocean at this time. However, as the deep overturning circulation develops, the density of the deep water starts to be affected. At 48 h, the water density increases at all depths within the radius of 100 km, and the maximum increase shifts to the center at depths of 20–50 m. Assuming an expansion modulus of 0.0003 and uniform salinity, the maximum equivalent temperature changes at the center are −3°C at a depth of 45 m, −1°C at 350 m and −0.3°C at 750 m. Outside 100 km radius, the density decreases between the depths of 30–120 m, with a maximum

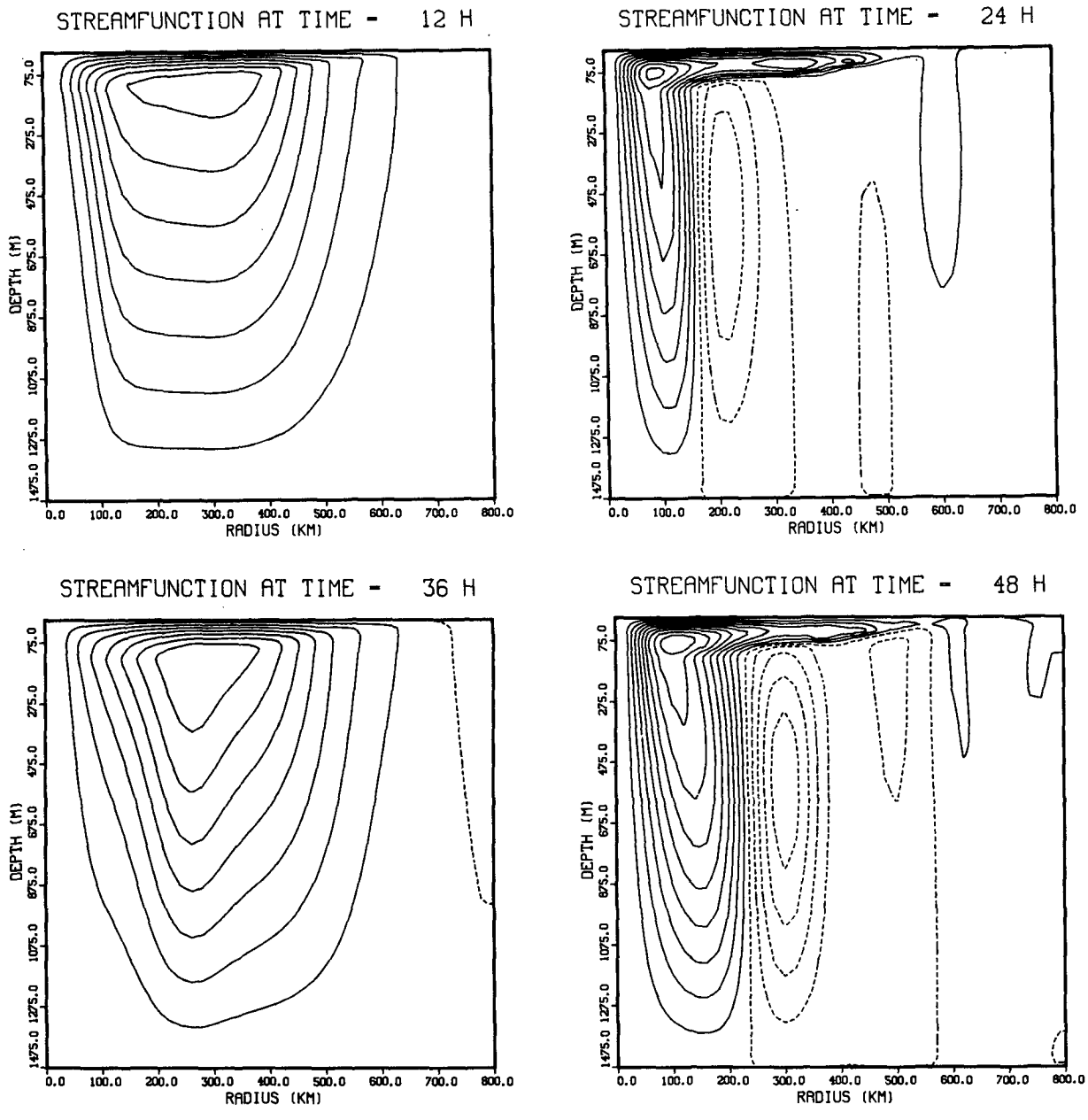

FIG. 4. Streamfunctions of the circulations on r–z plane at 12, 24, 36 and 48 h. Contour intervals are 8×10^{11} cm^3 s^{-1} for 12 and 36 h when the circulations are strong, and 2×10^{11} cm^3 s^{-1} for 24 and 48 h when the circulations are weak. Solid lines represent clockwise circulation on r–z plane, dashed lines represent counterclockwise circulations.

equivalent temperature increase of 0.45°C at 70–90 m and 180–300 km from the center. At $r > 330$ km, the warming extends to a great depth due to the prevailing downwelling there. The warming is only 10% of the cooling at the same depth near the center because the downwelling is weaker than the upwelling. The effect of the outward advection of the denser water by the radial current in the mixed layer is also apparent.

While there is no direct measurement of storm-induced density changes in the deep ocean, there is indication that Typhoon Tess (1975) left signatures deep in the Pacific. As shown by Figs. 3 and 4 in Pudov *et al.* (1978), the 17°C isotherm beneath the track of Tess was lifted about 40 m from a prestorm depth of 240 m. The temperature decrease due to a 40 m uplifting is close to 1°C. In fact, the water temperature is cooled by 0.5°C as deep as 440 m. Observations of Pudov *et al.* (1978) also showed that all isotherms in the central region below the mixed layer were uplifted by 40 m, which suggests a deep circulation in the plane perpendicular to the storm track as in this model.

The thermal response above the thermocline in this model is similar to other model simulations of the upper ocean response (e.g., O'Brien and Reid, 1967;

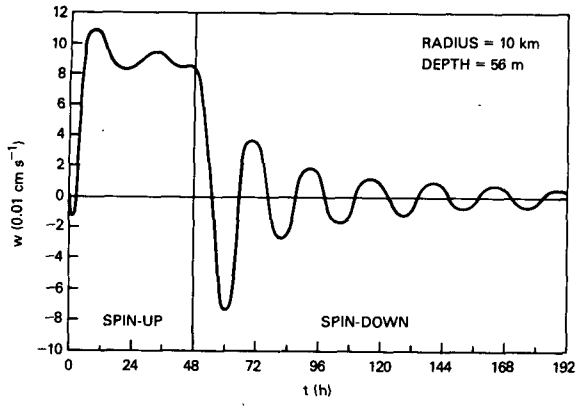

FIG. 5. Temporal variations of the vertical velocity at r = 10 km and d = 56 m for both the spinup and spindown.

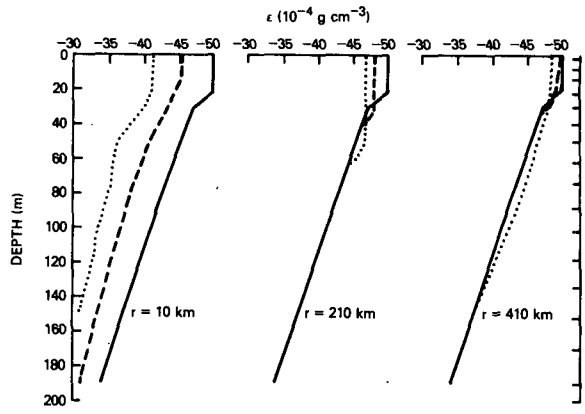

FIG. 7. Density profiles in the upper 200 m at radii of 10, 210 and 410 km for initial (solid line), 12 h (dash line) and 24 h (dot line). Ticmarks on the right indicate locations of grid points.

Chang and Anthes, 1979). By including several layers below the mixed layer, Price (1981) showed the warming below the thermocline due to mixing. As these are layer-type models, only mixing between layers can produce density changes. Besides, none of these earlier models extended to depths of more than 250 m. The density changes in the deep ocean in this model are solely caused by vertical motions, which are dynamically connected to the barotropic response.

c. *Mixed layer structure*

It is logical to define the mixed layer by a critical local Richardson number of unity because of the mixing closure in (18). At the radius of the maximum stress, the depth of the mixed layer increases from 30 m initially to 70 and 101 m at 24 and 48 h, respectively. Outside of 130 km radius, the depth of the mixed layer increases to 45 m.

The shears in the mixed layer are shown by the hodographs in Fig. 8. The shears in the tangential direction are mainly due to the surface water being constantly accelerated by the cyclonic stress during the spinup. Because the density stratification in the mixed layer is weakly stable and the vertical mixing is mostly mechanical, the existence of shears is necessary for downward momentum transfer. Contrarily, there is little shear in the radial flow in the mixed layer. The strongest outflow is located at 15 m below the surface in spite of the fact that the surface tangential flow is strongly super-gradient. This is because the surface stress has an inward component, opposite to the direction of the surface radial current. There is very strong

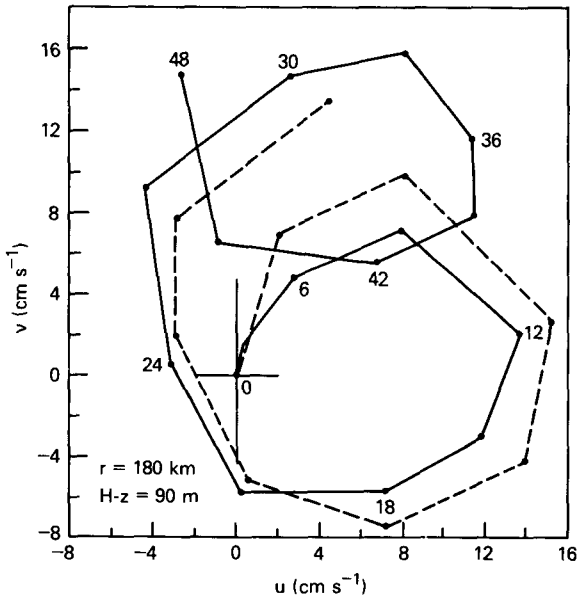

FIG. 6. Current vectors every 6 h at r = 180 km and depth of 90 m showing the inertial oscillation on the induced current. Current vectors of a rigid-lid, baroclinic model are linked with the dotted line.

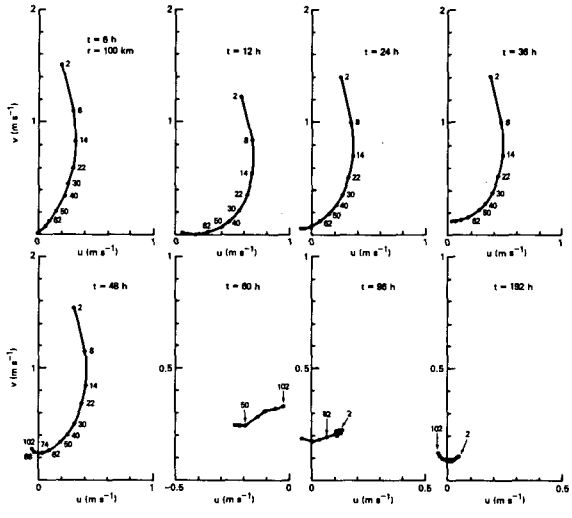

FIG. 8. Hodographs of induced currents at r = 100 km and depths of approximately 2, 8, 14, 22, 30, 40, 50, 62, 74, 88 and 102 m at 6, 12, 24, 36, 48, 60, 96 and 192 h. Note that the scale of the coordinates is decreased by a factor of two for 60, 96 and 192 h plots.

shear at the bottom of the mixed layer. At greater depth, the induced flows are of the barotropic kind with little shears. The predicted shear in the mixed layer presented here must be interpreted within the realm of the vertical mixing parameterization.

Figure 7 shows the density stratification in the upper 200 m of the ocean at 0, 24 and 48 h at three different radii. The figure demonstrates that the different dynamic response at each of the three radii produces a different thermal response. At the center, where upwelling is deep and strong, the density is increased at all depths. At r = 210 km, mixing is the dominant physical process, and the density is similar to that of a wind-stirred mixed layer. The prevailing downwelling at r = 410 km causes a warming much deeper than the mixed layer.

Among earlier models, only Gilbert's (1972) model has good vertical resolution to show poststorm mixed layer structure. A constant vertical mixing coefficient was used throughout his model and there was an artificial antimixing to restore the initial thermocline. As a consequence, the mixed layer never deepens, and the induced shear in Gilbert's model is eight times stronger than that in this model. For example, at the radius of the maximum stress, the surface current speeds in his model reached 4 m s^{-1} and vanished at the top of the thermocline at 25–30 m. Although the vertical shear of the mixed layer current under hurricanes are believed to be at the most moderate, no detailed post-hurricane mixed layer observations are available for comparison, unfortunately.

4. Barotropic response

The barotropic tangential velocity $[v]$ increases monotonically to reach a maximum of 19 cm s^{-1} at r = 80 km at 48 h (Fig. 9). The cyclonic $[v]$ is supported by a "low" in the mean mass field at small radii, which features a lowered surface and an increase in the mean density. The total tangential velocity $[v] + v'$ (Fig. 3) in the deep ocean at this radius is 13 cm s^{-1}; thus the barotropic response constitutes a major part of the deep response. (Note that v' is anticyclonic below the thermocline at almost all radii.) However, unlike the $[v]$, the barotropic radial velocity $[u]$ is oscillatory and is mostly inward except during the first few hours. Although the magnitude of $[u]$ is no more than 0.075 cm s^{-1}, which is much smaller than the outflow in the mixed layer (with maximum near 50 cm s^{-1}), the variation of $[u]$ allows the propagation of external gravity waves. It contributes to the total convergence–divergence that is responsible for the rise or fall of the surface. We will elucidate this point further.

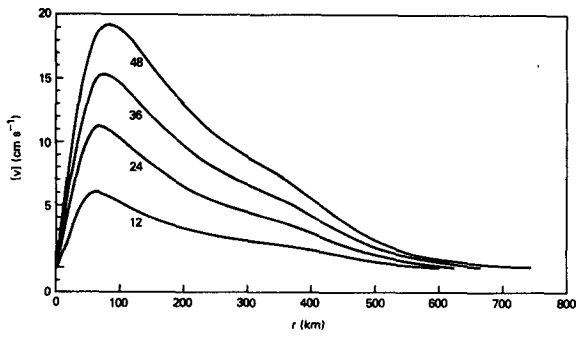

FIG. 9. Barotropic tangential velocities at 12, 24, 36 and 48 h.

The change of the free surface height is shown in Fig. 10. The surface falls continuously through the forcing period and reaches a maximum drop of 32 cm at 24 h and 57 cm at 48 h. The ocean surface rises beyond 380 km by as much as 6 cm at 48 h. This indicates a net mass divergence inside the radius of 380 km. (Because of incompressibility, a volume divergence is equivalent to a mass divergence.) There are three terms in the rhs of (17), the tendency equation of h. The first term represents the convergence due to the barotropic radial velocity $[u]$ in the mean water column H. The second term is the convergence of the surface radial velocity over the depth of h. The transport effect of the radial velocity at the surface is expressed in the third term. The values of the three terms in (17) for r = 0 at selected times are listed in Table 1.

The first and the second terms are always of the same magnitude but of the opposite signs, whereas the third term is at least two orders of magnitude smaller. At t = 1 h, the radial flow in the mixed layer is inward and water accumulates at the center. Because $[u]$ is positive, the first term becomes negative. The positive h and convergent surface radial velocity at this time give a positive value for the second term, which is a bit smaller in magnitude than the negative first term, and results in a decrease of h. The first two terms reverse signs at t = 4 h with a divergent $[u]$ and negative h. The same pattern remains throughout the forcing period. Given the positive mean divergence, negative surface divergence and negative dh/dt, the vertical velocity at r = 0 is upward at all depths above the ocean floor. However, it is negative at the surface, indicating a dropping water level. After 48 h, both terms diminish and become oscillatory.

The free surface height shown in Fig. 10, and the previous discussion are only pertinent for axisymmetric conditions. Under moving tropical cyclone, the change of ocean surface is not expected to remain symmetric. As it will be discussed in Part II, the surface height depression elongates along the storm path. Once the surface height is modified, however, the barotropic PGF can accelerate the deep ocean water.

5. Spindown

The thermal and dynamic structures of the ocean in the wake of a hurricane are very complicated, as pointed out by Chang and Anthes (1978) and others. The present two-dimensional model cannot properly simulate many of the wake effects. To spin down the ocean in the present model, we simply set the stress equal to zero after 48 h and integrate the model for

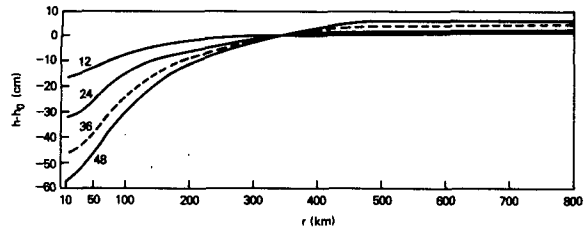

FIG. 10. Heights of the free surface at 12, 24 and 48 h.

another six days. The results should be interpreted cautiously because the sudden termination of wind stress may cause large inertial oscillations in currents (Gilbert, 1972). The purpose of the discussion here is to demonstrate the slow decay of the barotropic response.

After the surface wind stress is removed at 48 h, the supergradient tangential velocity in the mixed layer decreases immediately. The strong tangential shear in the mixed layer during the forcing period also disappears (Fig. 8). Similar to the mixed layer currents, the upwelling near the center weakens immediately after the removal of the stress (Fig. 5). The vertical motion changes directions with the inflow and outflow in the mixed layer with a period of approximately one day. As shown by Fig. 5, the vertical velocity at the depth of 56 m and r = 10 km experiences a rapid drop from 0.08 cm s^{-1} at 48 h to -0.08 cm s^{-1} at 54 h.

The recovery of the density field is equally as slow as the spindown of the momentum field. This is because the density field and the momentum field are nearly in balance. Six days after the removal of the surface stress, the density change near the center has only recovered by 30% from the peak at 48 h. The slow recovery of temperatures in near-surface ocean after Hurricane Eloise has been well documented (Johnson and Speer, 1978; Johnson and Withee, 1978; Fedorov *et al.*, 1979). Gill (1984) has also shown the slow horizontal and vertical dispersion of energy in the wakes of storms.

The spindown of the barotropic part of the response is very slow, in agreement with Geisler's (1970) linear theory. The model results indicate that the maximum depression of the free surface height only reduces from 57 cm at 48 h to 40.5, 33 and 26.7 after two, four and six days, respectively (Fig. 11). The tendency of h, and the values of the rhs terms of (17) during the spindown also fluctuate with time. As shown in Table 1 there is a decrease of magnitude of the dominant first and second terms after 48 h, which indicates the change of free surface height during spindown is much less vigorous than during spinup (Fig. 10). The mass–momentum adjustment seems to have reached a quasi-steady state after 144 h as h-h_0 oscillates around -32 cm.

The spindown of the vertical mean density $[\epsilon]$ due to perturbations is also rather slow (Fig. 11). The mean density change at r = 10 km is 70% of its maximum change at 96 h, 50% at 144 h and 33% at 192 h. The barotropic tangential velocity is nearly in gradient balance with the mass field after 144 h.

TABLE 1. Values of terms in free surface tendency equation (cm s^{-1}).

Time (h)	Mean convergence (Term 1) $\times 10^{-4}$	Surface convergence* (Term 2) $\times 10^{-4}$	Transport* (Term 3) $\times 10^{-6}$
1	−29.33	24.71	0.10
6	52.20	−58.29	−1.09
24	40.54	−41.05	−10.15
48	32.85	−35.06	−16.39
54	13.31	−11.96	−5.95
60	−2.70	2.95	11.86
96	5.36	−6.11	−1.31
144	8.45	−2.60	0.29
192	−3.33	−1.75	−0.13

* In the finite difference form, the second and the third terms are combined into a conserving flux form. Their separation here is for illustration purpose only.

6. Comparison with a one-layer, baroclinic model

For comparison with the free-surface model result, the one-layer, baroclinic model of Chang and Anthes (1979) is integrated under the same wind stress. The model, similar to other baroclinic models (e.g., O'Brien, 1967; Price, 1981), has a rigid surface and an inert bottom layer of infinite depth. The rate of the vertical mixing between the mixed and the bottom layers is proportional to the 1.5 power of the surface stress and inversely proportional to the depth and density anomaly of the mixed layer. An initial mixed layer depth of 50 m and a temperature jump of 5°C across the layer interface are assumed.

The spinup of the baroclinic model is qualitatively similar to that discussed in Section 3. Figure 12 compares the tangential velocities at the radius of maximum stress and the temperature changes at the center in the two models. The values of the tangential velocity in the baroclinic model, which represents the mean tangential velocity in the thermocline, lie between those at 10 and 50 m depths of the free-surface model. In both models, the velocity exhibits an initial speed-up

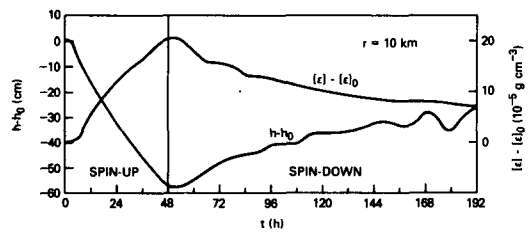

FIG. 11. Temporal variations at r = 10 km of the maximum depression of the free surface and the maximum barotropic density anomalies.

before 6 h, a decrease to about 18 h and a gradual increase toward 48 h. Outside the radius of the maximum stress, the induced current in the baroclinic model also has inertial oscillations similar to the free-surface model. The mixed layer current vectors at 180 km radius in the baroclinic model are plotted in Fig. 6.

The mean mixed layer temperature change in the baroclinic model is somewhat different from that in the free-surface layer model. In the free-surface model, temperature change can be induced by vertical mixing and vertical advection. In the baroclinic model, the effect of upwelling on the mixed layer temperature is indirect. Horizontal divergence in the baroclinic model causes first a shallowing of the mixed layer, which, through more effective mixing, can then induce cooling. Therefore, as shown in Fig. 12, the temperature decrease in the pure baroclinic model is slow before 24 h when the thermocline has not been sufficiently uplifted. The temperature then decreases rapidly between 24–48 h. On the other hand, the temperature in the free-surface model decreases rapidly in the first 24 h due to mixing and upwelling at both 10 and 50 m depths. Although final temperature changes differ only by 0.8°C at 48 h, the temporal variations in two models are quite different.

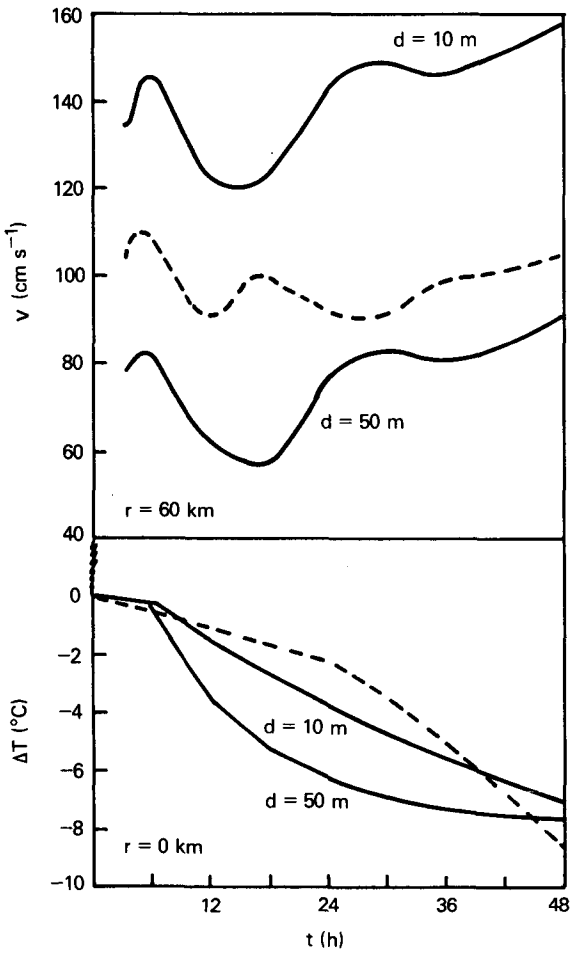

FIG. 12. Comparison with a flat-top, baroclinic model (dashed lines): (a) the tangential velocities at $r = 60$ km and (b) the temperature change at $r = 0$. Values at depths of 10 and 50 m from the free-surface model are plotted.

The one-layer baroclinic model can only resolve the mean mixed layer response to wind stress, whereas the free-surface model has 51 grid point in the vertical and therefore can resolve the current shears, temperature gradients and deep circulations. The comparison here only shows the vertical average response in the mixed layer of the free-surface layer. It can be concluded, nevertheless, that the mean mixed layer response simulated by the free surface model is qualitatively similar to earlier one-layer, pure baroclinic models.

7. Summary and discussion

The response in the shallow and deep ocean to the stress field of a stationary tropical cyclone has been studied with an axisymmetric, hydrostatic ocean model. The model differs from earlier models in that it contains the barotropic as well as baroclinic modes in the basic equations. Instead of assuming a flat ocean surface and an infinitely deep and motionless bottom layer, this model has a rigid bottom and a free surface.

Instead of using one grid point to represent the whole mixed layer, as in many earlier models, the vertical structure of the ocean is resolved with improved vertical resolution. There are 51 grid points in the vertical extending to a depth of about 1500 m using a stretched interval with a minimum of 5 m at the surface. With such a vertical resolution, the vertical turbulent mixing is parameterized based on a local Richardson number and a mixing length, which is assumed to be equal to the distance below the surface. Therefore, the vertical turbulent diffusivities depend on the local current shear, the local density stratification and the depth, $-z$. We have tested several turbulent Prandtl numbers. It turns out that the model results are not very sensitive to such details of the mixing formulation.

The model is numerically integrated for eight days. In the first two days, a constant and stationary surface stress similar to that of Hurricane Eloise is applied. The stress is then abruptly removed after two days and the ocean's poststorm adjustments are studied for six days. Notice that the atmospheric pressure force associated with the hurricane is ignored in this study. Results from supplementary numerical experiment indicate that the response of the ocean model to the pressure forcing of a typical hurricane is of a smaller magnitude. Rather, the barotropic response we study in this paper originates from the induced surface current, which is a baroclinic response. For simplicity, the thermal forcing of the hurricane has been neglected in this study.

The response in the upper ocean as revealed by this model is qualitatively similar to earlier studies. How-

ever, the model results indicate that the response reaches to a great depth, which has never been simulated before. We find that the tangential currents extend to the ocean bottom after 24 h, that the overturning occurs over nearly the entire water column as early as $t = 12$ h and the density (or temperature) in the deep ocean is modified by vertical motions. Because the vertical mixing cannot penetrate to such depth in a matter of a few hours, the dynamic response in the deep ocean must be "transmitted" by the barotropic pressure force. Thus the deep response is of the barotropic type. Based on the observational studies of Fedorov *et al.* (1979), Pudov *et al.* (1978), Hopkins (1982), Brooks (1983) and Shay and Elsberry (1985), it is evident that hurricanes do induce ocean response as deep as 400–500 m. Unfortunately, quantitative verification of model results is not possible at present, largely due to lack of deep sea observations.

There are many fine vertical structures in the ocean's response that are simulated by the model. We find the ocean surface is depressed by as much as 57 cm near the center due to the induced net mass divergence during spin up. (Note that the atmospheric low pressure associated with hurricanes will produce a bulge.) The forced tangential current has strong shear in the mixed layer with a maximum of about 2 m s^{-1} close to the surface at the radius of the maximum stress. However, there is very little shear in the mixed layer radial current that has a maximum of about 0.6 m s^{-1}. The maximum temperature decrease of 3°C at 20–50 m beneath the surface near the center is due to upwelling and mixing. The ocean layers just below the thermocline at large radii are warmed by downwelling and mixing.

The spindown of the model starts when the surface wind stress is suddenly removed. The poststorm ocean experiences inertial oscillations with large amplitudes over much of the depth of the ocean as the mass field and momentum field adjust. The inertial oscillations with a period of about one day are most obvious in the vertical velocity at the center (Fig. 5). The spindown, including the barotropic response, is very slow, in agreement with linear theory and observations.

In summary, this axisymmetric study illustrates several aspects of the ocean's response to tropical cyclones that have not been simulated before. Among the new findings are the significant barotropic response and the induced modification in the deep sea. These and other model results should be compared to conventional observations and eventually satellite altimeter measurements. We realize that a direct comparison of the model results to observations may not be realistic because of the two-dimensionality of the model. This and other constraints will be eliminated in a three-dimensional model. In such a model the stress field as well as the atmospheric pressure field will move with the storm, so that spinup and wake effects can be simulated more realistically. The three-dimensional results will be discussed in a forthcoming Part II.

Acknowledgments. I thank Dr. Keith Sashegyi for reading the manuscript and Mrs. Lorraine Ward for her help in preparing the manuscript. The work is supported by the U.S. Naval Research Laboratory Basic Research Program.

REFERENCES

Black, P. G., 1983: Ocean temperature changes induced by tropical cyclones. Ph.D. dissertation, The Pennsylvania State University, 278 pp.

Brooks, D. A., 1983: The wake of Hurricane Allen in the western Gulf of Mexico. *J. Phys. Oceanogr.*, **13,** 117–129.

Chang, S. W., 1984: A split-explicit integration method for ocean dynamic models. (in press) *Papers in Meteor. Res.*

——, and R. A. Anthes, 1978: Numerical simulations of the ocean's nonlinear baroclinic response to translating hurricanes. *J. Phys. Oceanogr.*, **8,** 468–480.

——, and ——, 1979: The mutual response of the tropical cyclone and the ocean. *J. Phys. Oceanogr.*, **9,** 128–135.

Elsberry, R. T., T. Fraim and R. Trapnell, Jr., 1976: A mixed layer model of the oceanic thermal response to hurricane. *J. Geophys. Res.*, **81,** 1153–1162.

Fedorov, K. N., A. A. Varfolomeev, A. I. Ginzburg, A. G. Zatsepin, A. Yu. Krasnopevtsev, A. G. Ostrovsky and V. E. Skylarov, 1979: Thermal reaction of the ocean on the passage of the Hurricane Ella. *Okeanologiya,* **19,** 656–661.

Geisler, J. E., 1970: Linear theory of the response of a two layer ocean to a moving hurricane. *Geophys. Fluid Dyn.*, **1,** 249–272.

Gilbert, K. D., 1972: The nonlinear transient response of a continuously stratified baroclinic ocean to stationary and transitory axially-symmetric atmospheric cyclones. Ph.D. dissertation, Texas A & M University.

Gill, A. E., 1984: On the behavior of internal waves in the wakes of storms. *J. Phys. Oceanogr.*, **14,** 1129–1151.

Greatbatch, R. J., 1983: On the response of the ocean to a moving storm: The nonlinear dynamics. *J. Phys. Oceanogr.*, **13,** 357–367.

Hopkins, C. K., 1982: Ocean response to hurricane forcing. M.S. thesis, Naval Postgraduate School, 89 pp.

Johnson, A., and G. A. Speer, 1978: Data report: Buoy observations during Hurricane Belle, August 1976. National Data Buoy Office, NSTL Station, MS, 22 pp.

——, and J. W. Withee, 1978: Ocean data buoy measurements of hurricane Eloise. *Mar. Technol. Soc. J.*, **12,** 14–20.

Kajiura, K. 1956: A forced wave caused by atmospheric disturbances in deep water. Tech. Rep. 133-1, Texas A & M University.

Kuo, H. H., and T. Ichiye, 1977: A numerical study of the response of a barotropic ocean to a moving hurricane. *Tellus,* **29,** 561–571.

Madala, R. V., and S. A. Piacsek, 1977: A semi-implicit numerical model for baroclinic oceans. *J. Comput. Phys.*, **23,** 167–178.

O'Brien, J. J., 1967: The nonlinear response of a two-layer baroclinic ocean to a stationary, axially-symmetric hurricane. Part II: Upwelling and mixing induced by momentum transfer. *J. Atmos. Sci.*, **24,** 208–215.

——, and R. O. Reid, 1967: The nonlinear response of a two-layer baroclinic ocean to a stationary, axially-symmetric hurricane. Part I: Upwelling induced by momentum transfer. *J. Atmos. Sci.*, **24,** 197–107.

Price, J. F., 1981: Upper ocean response to a hurricane. *J. Phys. Oceanogr.*, **11,** 153–175.

Pudov, V. D., A. A. Varfolomeev and K. N. Fedorov, 1978: Vertical structure of the wake of a typhoon in the upper ocean. *Okeanologiya,* **18,** 142–146.

Shay, L. K., and R. T. Elsberry, 1986: Observations of inertio-gravity waves in the wake of hurricane Frederic. Submitted to *J. Phys. Oceanogr.*

Suginohara, N., 1973: Response of a two-layer ocean to typhoon passage in the western boundary region. *J. Oceanogr. Soc. Japan,* **29,** 236–250.